Volume 1 | Number 1 | Jan 2013 | Pages 1–100

Polymer Chemistry

www.rsc.org/polymers

ROYAL SOCIETY OF CHEMISTRY

ROYAL SOCIETY OF CHEMISTRY

www.rsc.org/polymers

Journal Name

ARTICLE

Synthesis and characterization of poly(amino acid methacrylate)-stabilized diblock copolymer nano-objects

Vincent Ladmiral,[a,*] Alexandre Charlot,[b] Mona Semsarilar[c] and Steven. P. Armes[d,*]

Abstract Amino acids constitute one of Nature's most important building blocks. Their remarkably diverse properties (hydrophobic/hydrophilic character, charge density, chirality, reversible cross-linking etc.) dictate the structure and function of proteins. The synthesis of artificial peptides and proteins comprising main chain amino acids is of particular importance for nanomedicine. However, synthetic polymers bearing amino acid side-chains are more readily prepared and may offer desirable properties for various biomedical applications. Herein we describe an efficient route for the synthesis of poly(amino acid methacrylate)stabilized diblock copolymer nano-objects. First, either cysteine or glutathione is reacted with a commercially available methacrylate-acrylate adduct to produce the corresponding amino acid-based methacrylic monomer (CysMA or GSHMA). Well-defined water-soluble macromolecular chain transfer agents (PCysMA or PGSHMA macro-CTAs) are then prepared via RAFT polymerization, which are then chain-extended via aqueous RAFT dispersion polymerization of 2-hydroxypropyl methacrylate. In situ polymerization-induced self-assembly (PISA) occurs to produce sterically-stabilized diblock copolymer nano-objects. Although only spherical nanoparticles could be obtained when PGSHMA was used as the sole macro-CTA, either spheres, worms or vesicles can be prepared using either PCysMA macro-CTA alone or binary mixtures of poly(glycerol monomethacrylate) (PGMA) with either PCysMA or PGSHMA macro-CTAs. The worms formed soft free-standing thermo-responsive gels that undergo degelation on cooling as a result of a worm-to-sphere transition. Aqueous electrophoresis studies indicate that all three copolymer morphologies exhibit cationic character below pH 3.5 and anionic character above pH 3.5. This pH sensitivity corresponds to the known behavior of the poly(amino acid methacrylate) steric stabilizer chains.

Introduction

Amino acids are the fundamental building blocks of polypeptides and proteins. Using a palette of just 20 amino acids, Nature produces a plethora of polypeptides with precise sequence distributions that are capable of self-assembly in aqueous solution to form higher order structures (e.g. enzymes) and hence perform a wide range of biological functions. This complexity is fascinating and scientists from many disciplines are devoting their research careers to understanding the various mechanisms and design rules.[1] For polymer scientists in particular, acquiring a similar degree of control over the copolymer sequence as that achieved in Nature has become a highly desirable objective, because this would open up new avenues and undoubtedly lead to numerous applications.[2] For example, polypeptoids,[3] or poly(α-amino acids) derived from *N*-carboxyanhydrides (NCAs),[4,5] are arguably the protein and polypeptides biomimics that have been the subject of the most

intensive research. This effort has focused on polymers comprising amino acid motifs in the main chain, which are structurally analogous to naturally-occurring polypeptides. On the other hand, copolymers bearing amino acid side-chains may not form β-sheets or α-helices, but are still of significant interest for their capacity to undergo self-assembly in response to external stimuli such as pH or temperature, to bind to metal ions or to interact with other polyelectrolytes. Bio-inspired poly(2-oxazolines)[6] and polymers derived from amino acid-based vinyl monomers[7,8] are the best examples of this category. The latter class of polymers draws on early work by Kulkarni and Morawetz, who first reported the synthesis of *N*-amino acid (meth)acrylamides without using protecting group chemistry by reaction of (meth)acryloyl chloride with amino acids.[9] Similarly, Morcellet et al. studied the free radical polymerization behavior of alanine-, glutamic acid-, aspartic acid-, asparagine-, phenylalanine-, glycylglycine- and lysine-based methacrylamides and the effect of chiral centers on the solution,

aggregation and metal-complexing properties of the resulting amino acid-functional vinyl polymers.[10-19] Using a similar synthetic approach, Endo and co-workers studied the optical properties and aggregation of poly(meth)acrylamides based on single amino acids (e.g. L-leucine, L-phenylalanine, L-glutamic acid, L-tyrosine, methionine, proline, cysteine) or short polypeptides (methyl esters of L-leucyl-L-alanine, glycyl-L-leucyl-L-alanine, alanyl-L-leucyl-L-alanine, etc.).[20-29] North et al. prepared various methacrylates based on serine and serine di- or tripeptides.[30-33] Controlled polymerization techniques have also been used in this context.[34,35] For example, ring-opening metathesis polymerization (ROMP) was successfully employed to prepare a range of amino acid-functionalized homopolymers and block copolymers.[36-38] With regard to controlled radical polymerization formulations, atom transfer radical polymerization can be used to prepare similar copolymers.[39] However, reversible addition-fragmentation chain transfer (RAFT) polymerization seems to be preferred for such syntheses, presumably because of its superior tolerance of carboxylic acid functionality. McCormick and co-workers reported the aqueous RAFT polymerization of L- and D-alanine-base acrylamides, examined the chiroptical properties of the resulting polymers and also prepared shell cross-linked micelles via interpolyelectrolyte complexation.[40-43] Endo et al. used RAFT chemistry to prepare alanine-, and phenylalanine-containing polymers and block copolymers and examined both their thermo-responsive behavior and optical activity.[44-53] O'Reilly's group studied the stimulus-responsive self-assembly behavior of various amphiphilic diblock copolymers based on amino acid acrylamides. For example, *N*-acryloyl phenylalanine was used to prepare a pH-responsive copolymer capable of self-assembly in aqueous solution to form vesicles.[54,55] Amphiphilic star block copolymers containing phenylalanine methyl esters were synthesized and their potential use in enantiomer separation was investigated.[56] Block copolymers comprising poly(acrylic acid) and poly(*N*-acryloyl-(L)-phenylalanine), as well as the L- and D-leucine analogs, were used to prepare shell cross-linked micelles.[57,58] Finally, the same team developed several strategies to prepare polymeric nanoreactors based on a L-proline-based monomer; such nanoreactors were shown to efficiently catalyze aldol reactions.[59-63]

The self-assembly of amphiphilic diblock copolymers[64] allows the preparation of nano-objects such as spherical micelles,[65] worm-like micelles[66,67] and vesicles (a.k.a. polymersomes),[65,68-70] which have potential applications in nanomedicine, cell biology, electronics, energy and catalysis.[71-74] Block copolymer self-assembly is traditionally performed via post-polymerization processing of soluble copolymers using a solvent switch,[65] a pH switch[75] or thin film rehydration techniques.[76]

However, these processing techniques are typically only utilized in relatively dilute solution (< 1 %).[65-69,77] In contrast, the recent development of RAFT-mediated polymerization-induced self-assembly (PISA) formulations enables well-defined diblock copolymer nano-objects to be prepared directly at up to 25 % solids without recourse to any post-polymerization processing.[78,79]

Amongst the various amino acids, cysteine has been only seldom used for the side chain functionalization of polymers, presumably because its thiol group impairs radical polymerization unless masked.[80] However, in principle this functional group offers facile post-polymerization functionalization of polymers via thiol-ene and thiol-yne chemistries. This approach was recently exploited to functionalize polybutadiene,[81] and also to prepare new polyphosphoester-based micelles.[82]

Herein we exploit our well-exemplified RAFT aqueous dispersion polymerization protocol[78] to prepare a range of new poly(amino acid methacrylate)-based diblock copolymer nano-objects. In this approach, two amino acid-based methacrylates are readily prepared by reacting either cysteine or glutathione with a commercially available methacrylate/acrylate adduct. This thia-Michael addition proceeds selectively and quantitatively on a multi-gram scale in aqueous solution without recourse to protecting group chemistry, and does not require time-consuming purification steps. A systematic study of the effect of varying the diblock copolymer compositions is presented which enables the reproducible synthesis of pure copolymer morphologies (i.e. spheres, worms and vesicles). In addition, the thermo-responsive behavior of block copolymer worm gels and the pH-dependent behavior of these new nano-objects are examined. This article thus illustrates the use of amino acids to functionalize diblock copolymer self-assembled nanostructures obtained via PISA with two examples (cysteine and glutathione). It is important to note that, while the synthesis method is very general and could be used with biologically active oligopeptides, the amino acid- or peptide-derived monomers and polymers described herein do not retain the biological activity of their precursor.

Experimental

Materials and methods

3-(Acryloyloxy)-2-hydroxypropyl methacrylate (AHPMA), 2-hydroxyethyl acrylate (HEA), 4,4'-azobis(4-cyanovaleric acid) (ACVA, >98%), dimethylphenylphosphine (DMPP), trimethylsilyldiazomethane (2.0 M in diethyl ether), L-cysteine and L-glutathione were purchased from Aldrich and used as received. Glycerol monomethacrylate (GMA) was kindly donated by GEO Specialty Chemicals (Hythe, UK). 2-Hydroxypropyl methacrylate (HPMA, 97%) which comprises approximately 75% 2-hydroxypropyl methacrylate and 25 mol % 2-hydroxyisopropyl methacrylate was also purchased from Aldrich. According to HPLC analysis, this monomer contained ~ 0.1 mol % dimethacrylate impurity. Dichloromethane (DCM), 1,4-dioxane, diethyl ether, ethyl acetate, methanol and petroleum ether were all purchased from Fisher as HPLC grade solvents and used as received. Deionized water was used in all experiments. Silica gel 60 (0.0632-0.2 mm) was obtained from Merck (Darmstadt, Germany). NMR solvents (D$_2$O, CD$_3$OD, DMSO-d$_6$ and CDCl$_3$) were purchased from Goss Scientific Instruments Ltd. Dialysis membrane (MWCO = 1000) was purchased from Fisher Scientific (UK). 4-Cyano-4-(2-phenylethanesulfanylthiocarbonyl) sulfanyl-pentanoic acid (PETTC) was prepared as described previously.[78d]

Synthetic procedures

Synthesis of cysteine methacrylate (CysMA). L-Cysteine (15.13 g, 124.88 mmol) was placed in a round-bottomed flask and dissolved in deionized water (60 mL). 3-(Acryloyloxy)-2-hydroxypropyl methacrylate (29.43 g, 137.36 mmol) was then added to this aqueous cysteine solution. Finally, dimethylphenyl phosphine (17 µL, 1.25 x 10^{-4} mol) was added to the biphasic reaction mixture. After 2 h, the resulting monophasic reaction mixture was washed with ethyl acetate (2 x 50 mL) and dichloromethane (3 x 50 mL). The product was isolated as a pure white solid by freeze-drying from water overnight. Yield: 40.0 g, 95 %.
^{1}H NMR (400.13 MHz, D$_2$O, 298 K) δ (ppm): 1.89 (s, 3H, -*CH3*); 2.68-3.17 (m, 6H, -S-*CH2*-*CH2*-COO-,-S-*CH2*-CH(COO-)NH3+-); 3.79 (m, 1H, -*CH*OH); 3.90 (m, 1H, -*CH*(COO-)NH3+-); 4.20-4.30 (m, 4H, -*CH2*-CHOH-*CH2*-); 5.70 (s, 1H, vinyl), 6.13 (s, 1H, vinyl).

^{13}C NMR (400.13 MHz, D$_2$O, 298 K) δ (ppm): 17.3 (*CH3-*); 26.2 (-S-*CH2*-CH2); 32.0 (-S-*CH2*); 33.8 (-S-CH2-*CH2*); 53.4 (-CH2-*CH*OH-CH2-); 65.1, 65.2 (2C, -*CH2*-CHOH-*CH2*-); 66.8 (-*CH*(COO-)NH3+-); 127.3, 135.5 (2C, vinyl); 136.2 (2C, vinyl); 169.3, 172.7, 174.0 (3C, carbonyls).
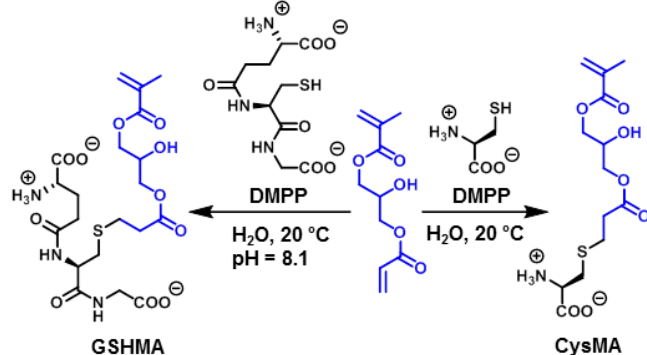(M+H+): calculated: 336.1117, found: 336.1105.
Elemental analysis: Calculated: C: 46.56 %; H: 6.31 %; N: 4.18 %; S: 9.56 %. Found: C: 46.10 %; H: 6.12 %; N: 4.20 %; S: 9.51 %.
Synthesis of glutathione methacrylate (GSHMA). A round-bottomed flask was charged with L-glutathione (10.02 g, 32.60 mmol), AHPMA (8.365 g, 39.05 mmol), DMPP (0.0194 g, 0.14 mmol) and water (65 mL) at 20°C. The biphasic reaction medium was vigorously stirred and cooled with an ice bath, and the pH was adjusted to 8.10.The emulsion-like mixture changed to a colorless aqueous solution within 50 min. The solution pH was adjusted to 6.90 and the reaction solution was then extracted using ethyl acetate (2 x 50 mL) and dichloromethane (3 x 50 mL). Traces of these organic solvents were then removed by distillation under reduced pressure. The glutathione methacrylate was not isolated, but instead kept as an aqueous solution (0.44 M, as determined via amine titration; crude yield = 95%).
^{1}H NMR (400.13 MHz, DMSO-d$_6$, 298K) δ (ppm): 1.95(s, 3H, –CH$_3$), 2.15 (dd, 2H), 2.50-2.54 (dt, 2H), 2.74-2.89 (m, 2H, 2H, 2H), 3.06-3.11(dd, 1H), 3.34 (t, 1H, OH), 3.71-3.80 (m, 4H), 4.20-4.25 (m, 4H), 5.77 (d, 1H), 6.18 (d, 1H), 8.19 (t, 1H), 8.52 (d, 3H). see Supplementary information (S1) for the fully assigned spectrum.
^{13}C NMR (400.13 MHz, DMSO-d$_6$, 298K) δ (ppm): 17.5 (1C), 26.3 (1C), 26.7 (1C), 31.5 (1C), 33.0 (1C), 34.2 (1C), 43.5 (1C), 54.2 (1C), 62.1 (1C), 65.3 (2C), 66.9 (1C), 127.3 (1C), 135.6 (1C), 169.3 (1C), 171.8 (1C), 174.0 (1C), 174.8 (1C), 176.1 (1C), 177.1 (1C).
(M+): calculated: 520.1601, found: 520.1591.

Scheme 1. Synthesis of the L-cysteine-based (CysMA) and glutathione-based (GSHMA) methacrylate monomers used in this work via thia-Michael addition

RAFT polymerization of CysMA. In a typical polymerization, a solution of CysMA (6.00 g; 17.899 mmol) in deionized water (50.0 g) was placed in a round-bottomed flask containing a magnetic flea, and a solution of PETTC (0.202 g, 5.96 x 10^{-4} mol) and ACVA (33.43 mg, 1.19 x 10^{-4} mol) in 1,4-dioxane (10.0 g) was added. This reaction solution was degassed via a nitrogen purge for 30 min and the flask was then placed in a preheated oil bath at 70 °C. The polymerization was quenched after 165 min (94 % conversion), and the crude polymer was purified by dialysis (MWCO = 1,000 Da) against deionized water and freeze-dried overnight. End-group analysis using ^{1}H NMR indicated a degree of polymerization of 31 (M_n (NMR) = 10 700 g mol^{-1}). This suggests a PETTC efficiency of 90 %. After derivatization (see below) the dried polymer was analyzed by DMF GPC (vs. PMMA standards), which gave: M_n = 24 200 g mol^{-1}, M_w = 26 800 g mol^{-1}, M_w/M_n = 1.11.

RAFT polymerization of GSHMA. In a typical polymerization, a round-bottomed flask was charged with a GSHMA solution (42.4 mL of a 0.441 M stock solution; 15.01 mmol), while a second round-bottomed flask was charged with PETTC (260.7 mg, 0.75 mmol), ACVA (43 mg, 0.15 mmol) and 1,4-dioxane (5 mL). Both solutions were degassed via a nitrogen purge. The 1,4-dioxane solution was then transferred into the aqueous solution via cannula. This round-bottomed flask was then placed in a preheated oil bath at 70 °C for 190 min. The resulting PGSHMA macro-CTA was purified by dialysis, first against 9:1 water/methanol and then against pure deionized water, and isolated by freeze-drying overnight (GSHMA conversion = 98 %). End-group analysis using ^{1}H NMR indicated a mean degree of polymerization of 24 (M_n (NMR) = 12 800 g mol^{-1}). This suggests a PETTC efficiency of 81 %. After derivatization (see below) the dried polymer was polymer was analyzed by DMF GPC (vs. PMMA standards), which gave: M_n = 9 800 g mol^{-1}, M_w = 11 800 g mol^{-1}, M_w/M_n = 1.20.
Similar reaction conditions were used to prepare PGSHMA macro-CTAs with mean DPs of 11 and 15.
RAFT polymerization of GMA. GMA (6.00 g, 37.46 mmol) was added to a round-bottomed flask containing a magnetic flea, PETTC (254.35 mg, 749 μmol) and ACVA (20.99 mg, 74.9 μmol). Ethanol (6.0 g) was added to this solution, which was then degassed via a nitrogen purge (N.B. the temperature was maintained below 10 °C using an ice bath during degassing). After 15 min, the round-bottomed flask was placed in a preheated oil bath at 70 °C. The polymerization was stopped after 190 min (90 % conversion), the polymer was purified by dialysis (MWCO = 1 000) against deionized water and freeze-dried overnight. DMF GPC analysis (vs. PMMA standards) gave M_n = 15 100 g mol^{-1}, M_w = 19 600 g mol^{-1} and M_w/M_n = 1.15. End-group analysis using ^{1}H NMR indicated a mean degree of polymerization of 55 (M_n = 9 100 g mol^{-1}), which suggests a PETTC efficiency of 82 %.

Polymerization-induced self-assembly (PISA). RAFT aqueous dispersion polymerizations were performed according to the following representative protocol. HPMA (188 mg, 1.31 mmol, target DP = 175) and deionized water (1.42 mL) were added to a sample vial containing a magnetic flea, PCysMA$_{31}$ macro-CTA (80 mg; 7.48 μmol) and ACVA initiator (200.0 μL of a 7.45 mM aqueous solution; macro-CTA/initiator molar ratio = 5.0). The reaction solution was degassed via a nitrogen purge for 15 min, and then placed in a preheated oil bath at 70 °C. The polymerization was quenched after 6 h (> 99 % conversion, as judged by ^{1}H NMR spectroscopy).
HPMA (375 mg, 2.60 mmol, target DP = 225) and deionized water (1.76 mL) were added to a sample vial containing a magnetic flea, PGMA$_{55}$ macro-CTA (100.0 mg, 10.42 μmol), PGSHMA$_{24}$ macro-CTA (14.81 mg, 1.16 μmol) and ACVA initiator (200.0 μL of a 11.66 mM aqueous solution; macro-CTA/initiator molar ratio = 5.0). The reaction solution was degassed by nitrogen bubbling for 15 min, and then placed in a preheated oil bath at 70 °C. The polymerization was quenched after 6 h (> 99 % conversion, as judged by ^{1}H NMR spectroscopy).
Similar polymerizations were conducted to target other PHPMA block DPs, which allowed access to either spherical, worm-like or vesicular copolymer morphologies.
Derivatization of PCysMA for GPC analysis. PCysMA (30.0 mg, 8.94 x 10^{-5} moles of CysMA) was added to a solution of acetic anhydride (91.32 mg, 8.94 x 10^{-4} mol) and triethylamine (18.1 mg, 1.79 x 10^{-4} mol) in acetonitrile (2.0 mL). Deionized water (1.0 mL) was then added to the suspension to obtain a homogeneous solution. Acylation was conducted at 20 °C for 60 min, then the reaction mixture was dialyzed against deionized water and freeze-dried overnight. The dried polymer was analyzed by DMF GPC (vs.

PMMA standards), which gave M_n = 24 200 g mol^{-1}, M_w = 26 800 g mol^{-1}, M_w/M_n = 1.11.

Derivatization of PGSHMA for GPC analysis. Michael addition of 2-hydroxyethyl acrylate (HEA) to PGSHMA was conducted as follows. Water (6.0 mL) was added to a vial containing PGSHMA$_{24}$ (200.0 mg, 0.38 mmol, 9.24 mmol amine equivalents) and 2-hydroxyethyl acrylate (144.80 µL, 27.72 mmol). The solution pH was adjusted to pH 10.5 and the vial was placed in an oil bath preheated to 50 °C. After 6 h, the pH was adjusted again to 10.5. The reaction was allowed to continue for a further 20 h. The product was then purified via dialysis against deionized water, and the protected polymer was isolated by freeze-drying overnight. Methylation of the carboxylic acid moieties was achieved as follows. HEA-modified PGSHMA$_{24}$ (50.0 mg) was dissolved in a 3:1 THF/water mixture (4.0 mL) and a yellow solution (0.2 mL) of trimethylsilyl diazomethane (2.0 M in diethyl ether) was added dropwise at 20 °C. On addition, nitrogen gas was evolved and the solution immediately became colorless. Further additions of trimethylsilyl diazomethane were made until the solution became yellow and no further nitrogen evolution was observed, and the solution was stirred for 6 h at 20 °C. The protected polymer was isolated by freeze-drying overnight after dialysis against first acetone and then deionized water. The dried polymer was analyzed by DMF GPC (vs. PMMA standards), which gave: M_n = 9 800 g mol^{-1}, M_w = 11 800 g mol^{-1}, M_w/M_n = 1.20).

Characterization methods

Gel Permeation Chromatography (GPC). Molecular weight distributions were determined using DMF GPC. The GPC set-up comprised two Polymer Laboratories PL gel 5 µm Mixed-C columns maintained at 60 °C in series with a Varian 390 LC refractive index detector. The flow rate was 1.0 mL min^{-1}, and the mobile phase contained 10 mmol LiBr. Ten near-monodisperse poly(methyl methacrylate) (PMMA) standards (M_p = 625 to 618 000 g mol^{-1}) were used for calibration.

NMR Spectroscopy. All ^{1}H NMR and ^{13}C NMR spectra were recorded in CD$_3$OD, DMSO-d$_6$ or D$_2$O using either a 250 MHz Bruker Avance 250 or a 400 MHz Bruker Avance 400 spectrometer.

Transmission Electron Microscopy. TEM images were acquired using a Philips CM100 instrument operating at 100 kV. To prepare TEM grids, 5.0 µL of a dilute aqueous copolymer solution was placed onto a carbon-coated copper grid, stained using uranyl formate, and then dried under ambient conditions.

Dynamic Light Scattering. DLS measurements were conducted at 25 °C at a fixed scattering angle of 173° using a Malvern Instruments Zetasizer Nanoseries instrument equipped with a 4 mW He-Ne laser operating at 633 nm, an avalanche photodiode detector with high quantum efficiency, and an ALV/LSE-5003 multiple tau digital correlator electronics system. The intensity-average diameter and polydispersity of the diblock copolymer particles were calculated by cumulants analysis of the experimental correlation function using Dispersion Technology Software version 6.20.
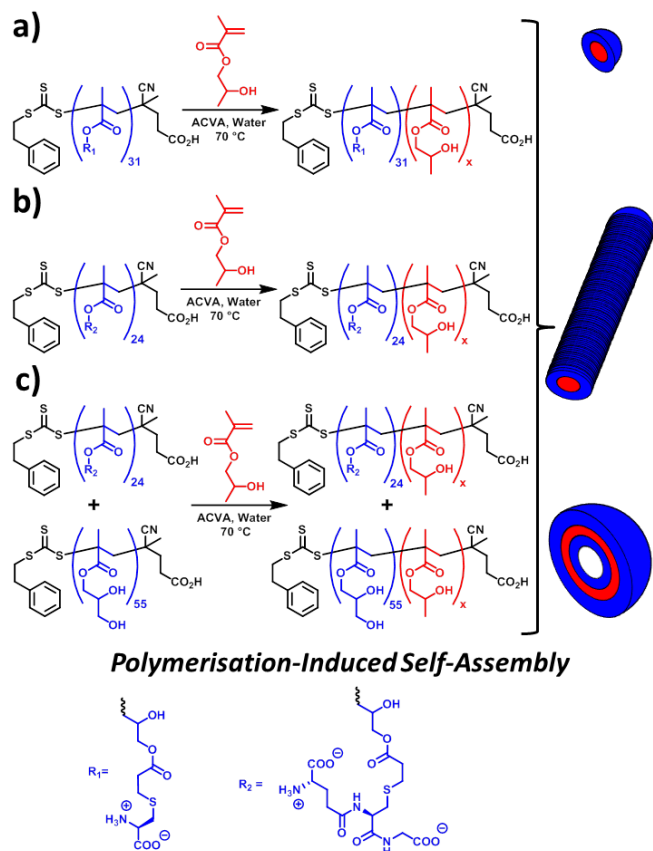
Rheology Studies. The storage modulus (G') and loss modulus (G") curves for selected diblock copolymer worm gels were determined using a TA Instruments AR-G2 rheometer equipped with a Peltier heating/cooling plate. A cone-and-plate geometry (40 mm, 2° aluminum cone) was used for these measurements. Temperature sweeps were conducted at a fixed strain of 1.0 % using an angular frequency of 1.0 rad s^{-1}. Stepwise sweeps were conducted at increments of 1.0 °C, using an equilibration time of 3 min for each step and an equilibration time of 5 minutes at 25 °C and 1 °C.

Results and Discussion

Monomer syntheses. Two novel ionic methacrylic monomers were prepared via thia-Michael addition. Phosphine-catalyzed nucleophilic addition[83] of a thiol to an acrylate is fast, highly selective and atom-efficient; this chemistry was recently utilized to synthesize poly(N-isopropyl acrylamide)[84] and polyethylene macromonomers,[84] as well as a glycomonomer.[78f] In the present work, two thiol-functional precursors, L-cysteine and L-glutathione, were reacted in turn with 3-(acryloyloxy)-2-hydroxypropyl methacrylate (AHPMA) to afford the desired methacrylic monomers in very high yields within short reaction times under mild conditions (Scheme 1). These reactions were performed in water at 20 °C and the crude monomers were readily purified by simply washing with ethyl acetate and dichloromethane. The L-cysteine-based methacrylate (CysMA) was isolated as a white powder by freeze-drying the aqueous reaction solution. In the case of the L-glutathione-derived methacrylate (GSHMA), a similar protocol was employed, but the solution pH was maintained between 7 and 9 throughout the reaction via addition of dilute NaOH. The initial pH of the glutathione solution is 4, but thia-Michael addition occurs much faster when the thiol group and the phosphine catalyst are present in their deprotonated thiolate and phosphine forms. The respective pK$_a$ values for the DMPP catalyst and the glutathione are 6.80 and 8.75. Unfortunately, freeze-drying of the aqueous GSHMA solution led to a white powder which could not be dissolved in water, DMSO or DMF. Thus this monomer was instead stored as an aqueous solution, the concentration of which was determined by titration of the glutathione amine group (see Figure S2).

RAFT polymerization of CysMA and GSHMA monomers. RAFT polymerization of each of these two monomers was conducted in turn in water/dioxane mixtures using a PETTC RAFT agent. High monomer conversions (> 94%) were achieved with good molecular weight control (Figures S3 and S4). Mean degrees of polymerization (DP) were calculated by end-group analysis using ^{1}H NMR spectroscopy, assuming that every polymer chain contained a PETTC-based end-group. The resulting PCysMA$_{31}$ and PGSHMA$_{24}$ homopolymers required derivatization prior to DMF GPC analysis. The amine groups of PCysMA$_{31}$ were acetylated using acetic anhydride. The DMF GPC chromatogram (Figure S3a) of the acetylated PCysMA$_{31}$ indicated a narrow molecular weight distribution (M_w/M_n = 1.11). The small shoulder at higher molecular weight suggests that some low degree of bimolecular termination occurred during the RAFT polymerization. In the case of PGSHMA$_{24}$, the amine moieties were alkylated via Michael addition of 2-hydroxyethyl acrylate while the carboxylic acid groups were methylated using trimethylsilyl diazomethane. DMF GPC analysis of the derivatized polymer (Figure S3b) also confirmed a narrow molecular weight distribution (M_w/M_n = 1.20).

Polymerization-Induced Self-Assembly (PISA). These novel PCysMA$_{31}$ and PGSHMA$_{24}$ macro-CTAs were then chain-extended in turn using 2-hydroxypropyl methacrylate (HPMA) under RAFT aqueous dispersion polymerization conditions (see Scheme 2).[78] As previously observed with other water-soluble macro-CTAs, these syntheses were accompanied by greater turbidity as the HPMA polymerization progressed.[78] This increase in turbidity corresponds to the onset of copolymer aggregation and is accompanied by an enhanced rate of polymerization, which is believed to be the result of preferential partitioning of unreacted HPMA monomer within the growing PHPMA-core micellar aggregates.[78,79a] In all cases, the HPMA polymerization proceeded to high conversion (> 98 % as judged by ^{1}H NMR).

Scheme 2. Preparation of diblock copolymer nano-objects via polymerization-induced self-assembly (PISA) of 2-hydroxypropyl methacrylate (HPMA) using: (a) PCysMA$_{31}$ RAFT macro-CTA, (b) PGSHMA$_{24}$ RAFT macro-CTA and (c) a binary mixture of PGMA$_{55}$ and PGSHMA$_{24}$ RAFT macro-CTAs.

Like earlier RAFT PISA formulations, the final morphology of the resulting PCysMA$_{31}$-PHPMA$_x$ diblock copolymer nano-objects depended on the target DP of the hydrophobic PHPMA block and the total solids content. These two parameters were systematically varied in order to construct a non-equilibrium phase diagram that serves as a convenient 'road map', thus enabling the reproducible preparation of morphologically pure nano-objects, e.g. well-defined spherical nanoparticles, worms or vesicles (Figure 1a). Representative TEM images for the various nano-objects are shown in Figure 1b. Unlike the zwitterionic PCysMA, PGSHMA has anionic character since it possesses two carboxylic acid groups and one amine group. This has important consequences for PISA syntheses: only a spherical morphology was obtained over the entire phase space ($100 < DP_{PHPMA} < 300$; total solids content = 10-20 % w/w) when using the PGSHMA$_{24}$ macro-CTA (see Figure S5). Figure 2 shows a representative TEM image of these PGSHMA$_{24}$-PHPMA$_{100-300}$ nanoparticles. In this case, lateral repulsion between neighboring anionic PGSHMA coronal chains prevents the formation of so-called 'higher order' morphologies such as worms and vesicles. A similar problem has been reported when employing other polyelectrolytic macro-CTAs for the RAFT aqueous dispersion polymerization of HPMA.[78d-e] A series of PGSHMA$_{24}$-PHPMA$_x$ diblock copolymers were synthesized under PISA conditions in the presence of NaCl in an attempt to screen the electrostatics and hence facilitate more efficient packing of the anionic PGSHMA stabilizer chains within the coronal layer of the sterically-stabilized nanoparticles. This strategy has been previously used by Charleux et al. for RAFT aqueous emulsion polymerization[79g] and by Semsarilar et al. for RAFT aqueous dispersion polymerization.[78d-e] However, only spherical nanoparticles were obtained in the present study (see Figure S6). GSHMA has a relatively high monomer mass (543 g mol^{-1}) and consequently each residue of the PGSHMA stabilizer chains occupies a significantly larger molecular volume than a HPMA repeat unit in the core-forming PHPMA block.
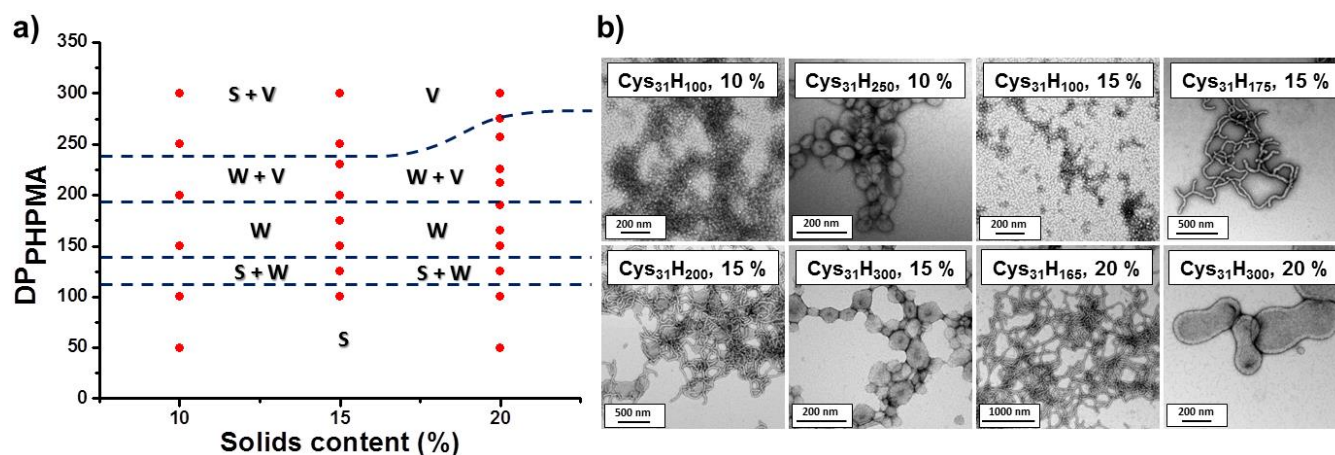

Figure 1. (a) Phase diagram constructed for PCysMA$_{31}$–PHPMA$_x$ diblock copolymer nano-objects prepared by RAFT aqueous dispersion polymerization at 70 °C. The target PHPMA DP and the total solids content were systematically varied and the *post mortem* copolymer morphologies obtained at > 98 % HPMA conversion were determined by TEM. N.B. **S**, **W**, and **V** denote spheres, worms and vesicles, respectively. (b) Representative TEM images obtained for PCysMA$_{31}$–PHPMA$_x$ (denoted Cys$_{31}$–H$_x$ for brevity) diblock copolymer nano-objects prepared by RAFT aqueous dispersion polymerization of HPMA at 70 °C. The target diblock composition and copolymer % solids contents are indicated on each image.
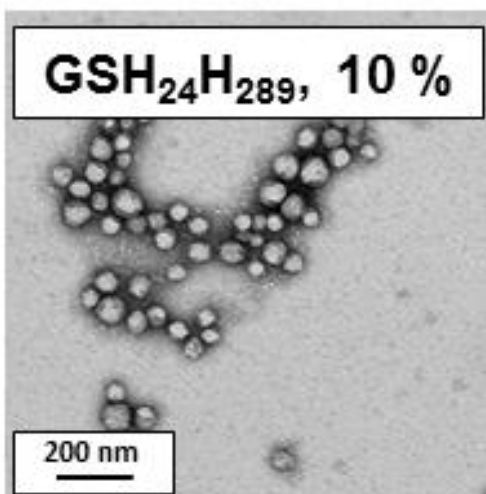
Journal Name

ARTICLE

Figure 2. Representative TEM image obtained for PGSHMA$_{24}$–PHPMA$_{289}$ diblock copolymer spheres prepared at 10 % w/w solids via RAFT aqueous dispersion polymerization of HPMA at 70 °C. (PGSHMA and PHPMA are denoted 'GSH' and 'H' respectively for brevity)

The geometric packing model invoked by Israelachvili for small molecule surfactants,[85] wherein the relative volume fractions of the hydrophilic and hydrophobic components dictate self-assembly, has been applied to block copolymer nano-objects.[69,86] Previous studies by Armes and co-workers confirmed that, when high molar mass monomers such as lauryl methacrylate[79f] or 2-(methacryloyloxy)ethyl phosphorylcholine (MPC)[78c] are used as the stabilizer block in RAFT dispersion polymerization, highly asymmetric diblock copolymer compositions are required to access the worm or vesicle phases. Thus the volume fraction of even the relatively short PGSHMA$_{24}$ block might be too high to allow formation of worms and vesicles. Shorter PGSHMA (PGSHMA$_{15}$ and PGSHMA$_{11}$) macro-CTAs were also synthesized and evaluated as stabilizers for RAFT PISA syntheses. However, this strategy also failed to provide access to either worms or vesicles. Only spherical aggregates were observed (see Figure S7) for PHPMA target DPs of 100, 150 or 200 regardless of the solids contents utilized for these PISA syntheses (10-20%). Finally, a fourth strategy involving the use of binary mixtures of PGSHMA$_{24}$ and PGMA$_{55}$ [where PGMA = poly(glycerol monomethacrylate)] macro-CTAs was examined. This approach had already proven to be successful when using other polyelectrolytic water-soluble polymers such as poly(potassium 3-sulfopropyl methacrylate) (PKSPMA)[78d] or quaternized poly(2-(dimethylamino)ethyl methacrylate) (PQDMA).[78e] This approach proved to be fruitful: a 1:9 binary mixture of PGSHMA$_{24}$ and PGMA$_{55}$ macro-CTAs yielded well-defined spheres, worms or vesicles (Figure 3b). Systematic variation of the mean target degree of polymerization of the core-forming PHPMA block allowed construction of a detailed phase diagram (see Figure 3a), which enables pure copolymer morphologies to be prepared reproducibly. This versatile approach was also successful when using 1:9 binary mixtures of PCysMA$_{31}$ and PGMA$_{55}$ macro-CTAs (see Figure 4).
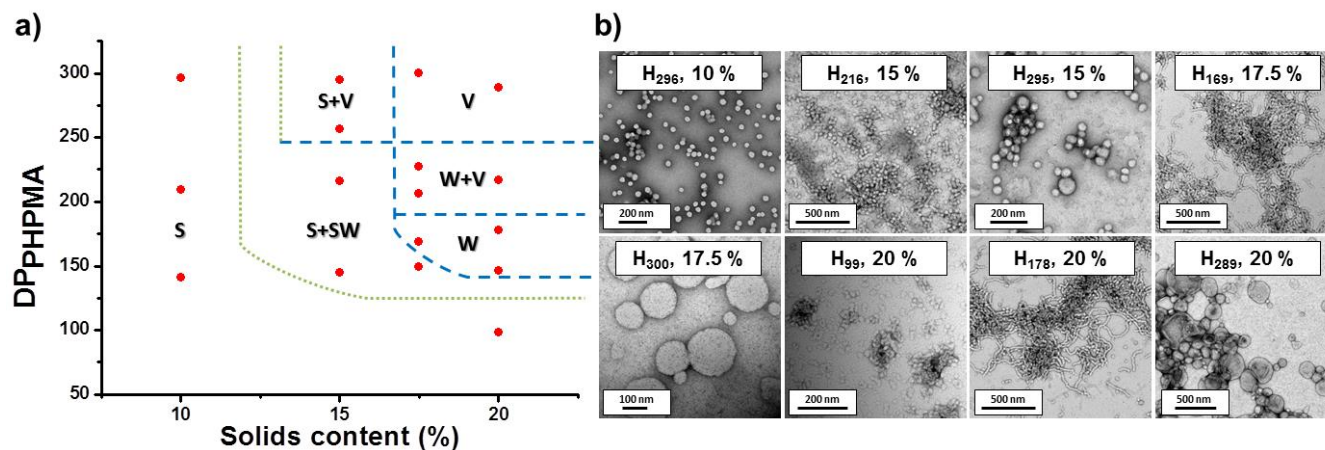
Journal Name

ARTICLE

Figure 3. (a) Phase diagram constructed for (1:9 PGSHMA$_{24}$ + PGMA$_{55}$)–PHPMA$_x$ diblock copolymer nano-objects prepared by RAFT aqueous dispersion polymerization at 70˚C. The target PHPMA DP and the total solids content were systematically varied and the *post mortem* copolymer morphologies obtained at > 98 % HPMA conversion were determined by TEM. N.B. **S, SW, W, V** denote spheres, short worms, worms and vesicles, respectively. Blue dashed lines and green dotted lines indicate tentative phase boundaries. (b) Representative TEM images obtained for (1:9 PGSHMA$_{24}$ + PGMA$_{55}$)–PHPMA$_x$ diblock copolymer nano-objects prepared by RAFT aqueous dispersion polymerization of HPMA at 70 °C. The target DP for the PHPMA block (herein denoted by 'H' for brevity) and the copolymer solids content % is indicated on each image.

Figure 4. (a) Phase diagram constructed for (1:9 PCysMA$_{31}$ + PGMA$_{55}$)–PHPMA$_x$ diblock copolymer nano-objects prepared by RAFT aqueous dispersion polymerization at 70˚C. The target PHPMA DP and the total solids content were systematically varied and the *post mortem* copolymer morphologies obtained at > 98 % HPMA conversion were determined by TEM. N.B. **S, SW, W, V** denote spheres, short worms, worms and vesicles, respectively. The blue dashed lines and green dotted lines indicate tentative phase boundaries. (b) Representative TEM images obtained for (1:9 PCysMA$_{31}$ + PGMA$_{55}$)–PHPMA$_x$ copolymer nano-objects prepared by RAFT aqueous dispersion polymerization of HPMA at 70 °C. The target DP for the PHPMA block (herein denoted by 'H' for brevity) and the copolymer solids content % is indicated on each image.
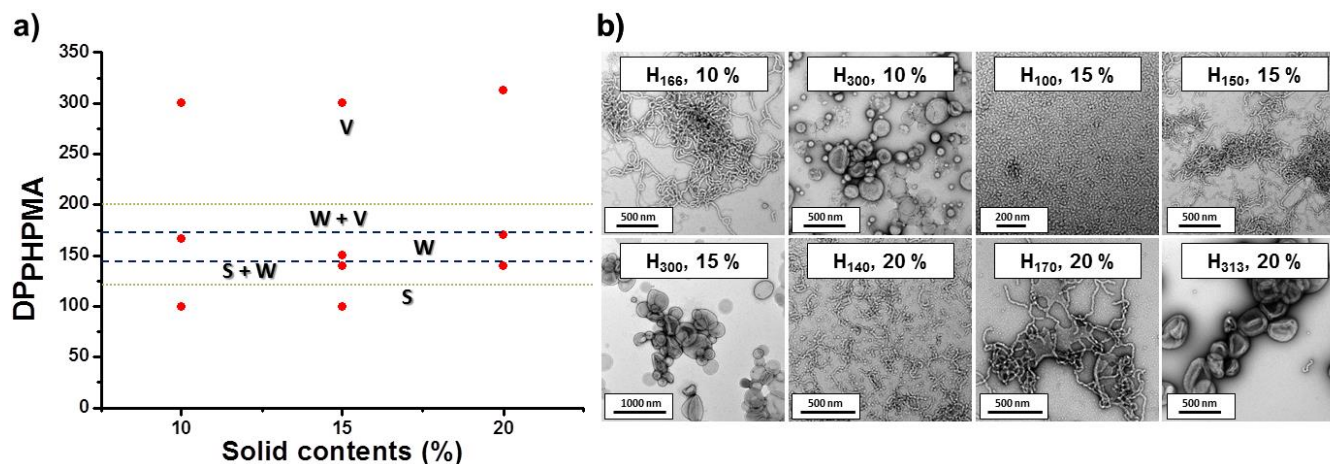
Worm-to-sphere thermal transition. Previous studies have shown that diblock copolymer worms comprising PHPMA as the core-forming block are thermo-responsive, undergoing a reversible morphological worm-to-sphere transition on lowering the solution temperature from 20 °C to around 5 °C.[78f,87] However, the PCysMA$_{31}$–PHPMA$_x$ diblock copolymer worms prepared in the present study did not exhibit any discernible change in morphology on cooling from 25 °C to 1 °C. Presumably, *attractive* electrostatic

interactions between neighboring zwitterionic stabilizer chains oppose a reduction in the packing parameter and so prevent the transformation of worms into spheres. This hypothesis is supported by the observation that 1:9 binary mixtures of (PCysMA$_{31}$ + PGMA$_{55}$) and (PGSHMA$_{24}$ + PGMA$_{55}$) macro-CTAs each exhibited a thermally-induced worm-to-sphere transition on cooling, as shown in Figure 5. More specifically, aqueous dispersions of (1:9 PCysMA$_{31}$ + PGMA$_{55}$)-PHPMA$_{166}$ and (1:9 PGSHMA$_{24}$ + PGMA$_{55}$)-PHPMA$_{178}$ worms[88] formed translucent free-standing gels at 10-20% w/w solids, similar to the worm gels previously reported for aqueous dispersions of PGMA$_{54}$-PHPMA$_{140}$ and (1:9 PGalSMA$_{34}$ + PGMA$_{51}$)-PHPMA$_{150}$ diblock copolymers (where GalSMA is a galactose-based methacrylate).[78f,87] However, cooling from 20 °C to 1°C led to rapid degelation, with the worm gel phase being reformed on returning to 20 °C. Rheology studies were undertaken to examine this thermo-reversible transition (see Figures 5a and 5c).
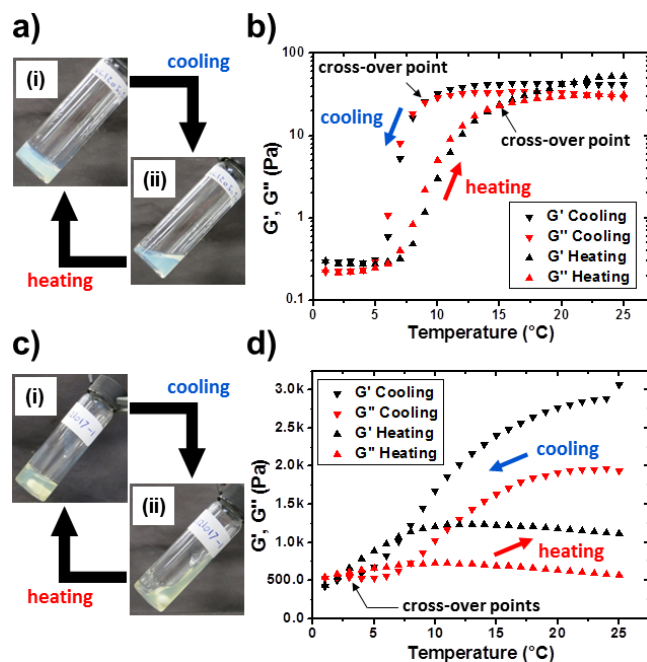

Figure 5. (a) Digital photographs recorded for a 10% w/w aqueous dispersion of (1:9 PCysMA$_{31}$ + PGMA$_{55}$)-PHPMA$_{166}$ worms recorded at (i) 20 °C (free-standing gel) and (ii) 1 °C (free-flowing fluid). (b) Variation of storage modulus (G', black symbols) and loss modulus (G'', red symbols) for the same 10% w/w diblock copolymer worm gel during thermal cycling in 1 °C increments: (i) cooling from 25 °C to 1 °C (G' = inverted black triangles, G'' = inverted red triangles) and (ii) subsequent warming to 25 °C in 1 °C increments (G' = black triangles, G'' = red triangles). (c) Digital photographs recorded for a 20% w/w aqueous dispersion of (1:9 PGSHMA$_{24}$ + PGMA$_{55}$)-PHPMA$_{178}$ worms recorded at (i) 20 °C (free-standing gel) and (ii) 1 °C (free-flowing fluid). (d) Variation of storage modulus (G', black symbols) and loss modulus (G'', red symbols) for the same 20% w/w diblock copolymer worm gel during thermal cycling in 1 °C increments: (i) cooling from 25 °C to 1 °C (G' = inverted black triangles, G'' = inverted red triangles) and (ii) subsequent warming from 1 °C to 25 °C in 1 °C increments (G' = black triangles, G'' = red triangles).

More specifically, the temperature dependence of the storage (G') and loss (G'') moduli was monitored (Figures 6b and 6f) for two aqueous worm dispersions: (1:9 PCysMA$_{31}$ + PGMA$_{55}$)-PHPMA$_{166}$

at 10% w/w, and (1:9 PGSHMA$_{24}$ + PGMA$_{55}$)-PHPMA$_{178}$ at 20% w/w solids. In the case of the (1:9 PCysMA$_{31}$ + PGMA$_{55}$)-PHPMA$_{166}$ dispersion, G' exceeds G'' between 25 °C and 9 °C, which indicates the formation of a soft viscoelastic gel. Below 9 °C, G' is reduced by two orders of magnitude and crosses the G'' curve; this indicates the formation of a free-flowing viscous liquid at sub-ambient temperatures (see Figure 5b). During the heating cycle, cross-over occurs at a slightly higher critical gelation temperature of 15 °C. Similar hysteresis was also observed for a 10% w/w aqueous dispersion of PGMA$_{55}$-PHPMA$_{178}$ worms.[87] Above 15 °C, G' and G'' return to their approximate original values and a free-standing translucent gel is reformed. The molecular origin for this worm-to-sphere transition is the well-known thermo-sensitive nature of the PHPMA block,[87] which leads to subtle variation in the hydration of these weakly hydrophobic chains, thus causing a shift in the packing parameter that dictates the overall copolymer morphology.[87,89] The 20% w/w aqueous dispersion of (1:9 PGSHMA$_{24}$ + PGMA$_{55}$)-PHPMA$_{178}$ worms behaves slightly differently. This aqueous dispersion also undergoes a thermal transition (see Figure 5c). At 20 °C, it forms a free-standing, almost transparent gel. When cooled to 1 °C, this gel flows like a viscous liquid and quickly regels as soon as it is allowed to warm up. The changes in G' and G'' observed during 25 °C - 1 °C - 25 °C thermal cycles are presented in Figure 5d. During cooling, G' exceeds G'' from 25 °C to 3 °C, cross-over occurs at 3 °C and G' is less than G'' between 3 °C and 1 °C. During this part of the cycle, both moduli are reduced by one order of magnitude. On heating, cross-over occurs at 2.5 °C, but G' only increases up to 1000 Pa at 25 °C, compared to an original G' of 2800 Pa at 25 °C. The experimental time scale may be simply too short to allow the gel to recover its original structure. Indeed, worm gel formation can sometimes be relatively slow, with gel properties gradually evolving over time. Figure S9 presents the rheological data for a similar thermal cycle performed on a similar aqueous worm gel. These studies indicate that the dispersion undergoes a transition from a strong viscoelastic gel into a highly viscous liquid at around 3 °C. However, at this relatively high concentration (20 % w/w), the worms may not be fully transformed into spheres. Temperature-dependent DLS studies of this change in morphology conducted on a 1.0 % w/w aqueous worm dispersion are consistent with the above visual observations and rheological data (see Figures S11a and S11b). A more detailed study of the complex thermo-responsive behavior of these new worm gels will be published elsewhere in due course.

Surface charge studies

Zeta potential vs. pH and intensity-average diameter vs pH curves were recorded for selected diblock copolymer nano-objects using aqueous electrophoresis and DLS, respectively. Measurements were performed on a series of dispersions each prepared at the desired pH. The zeta potential vs. pH curves (see Figures 6a and 6b) show that PCysMA- and PGSHMA-stabilized spheres possessed cationic character below pH 3.5 or pH 3.0, respectively, with both becoming more anionic at higher pH. Initially, the PCysMA-stabilized spheres were colloidally stable, but they aggregated when the solution pH approached the IEP, with full redispersion being observed between pH 4 and pH 6. Above pH 6, aggregation was again observed. This aggregation might be associated with the known chemical instability[90] of PCysMA in alkaline media: the deprotonated amine groups produced above pH 9 react with ester carbonyl groups, leading to side-chain elimination and possibly cross-linking. Similar pH-dependent chemical degradation has been previously reported for poly(2-aminoethyl methacrylate) in dilute aqueous solution.[91]
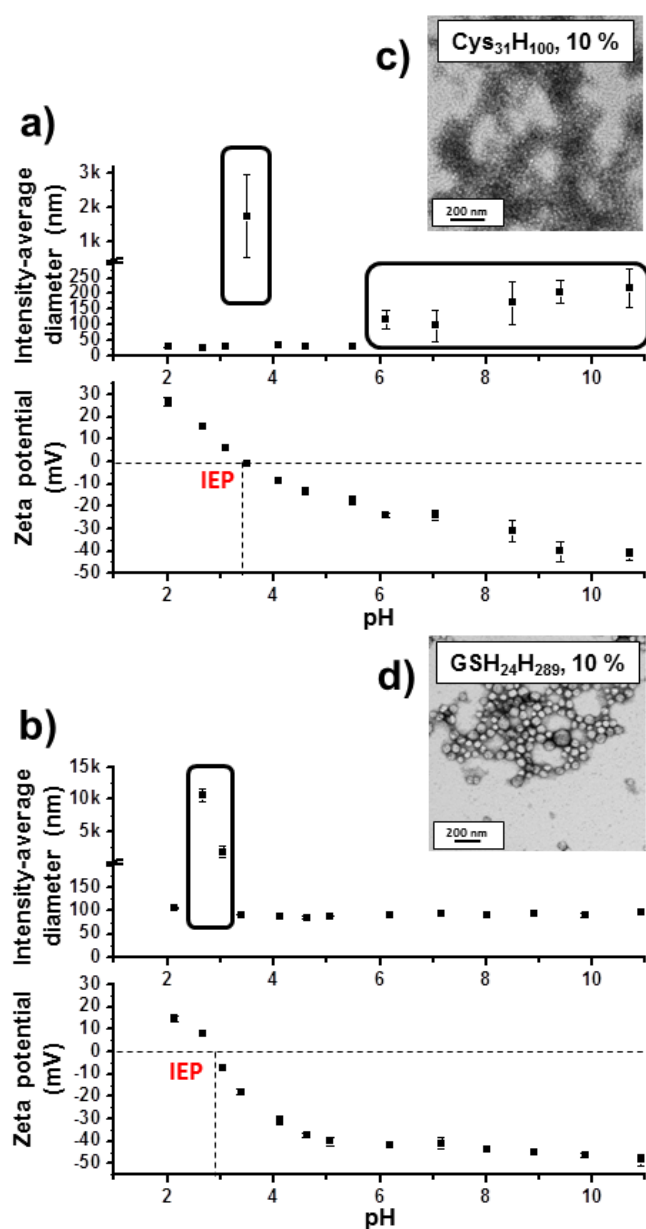
Figure 6. Variation of zeta potential and intensity-average diameter with pH for: (a) PCysMA$_{31}$-PHPMA$_{100}$ spheres; and (b) PGSHMA$_{24}$–PHPMA$_{289}$ spheres. Each data point was obtained for an individual dispersion diluted to obtain the desired final pH. (c) and (d): Representative TEM micrographs obtained for PCysMA$_{31}$-PHPMA$_{100}$ spheres and PGSHMA$_{24}$–PHPMA$_{289}$ spheres respectively.

Spherical nanoparticles prepared using the PGSHMA$_{24}$ macro-CTA also exhibited colloidal instability when the pH of the aqueous dispersion approached the IEP, but in this case no further instability was observed between pH 7 and pH 11.
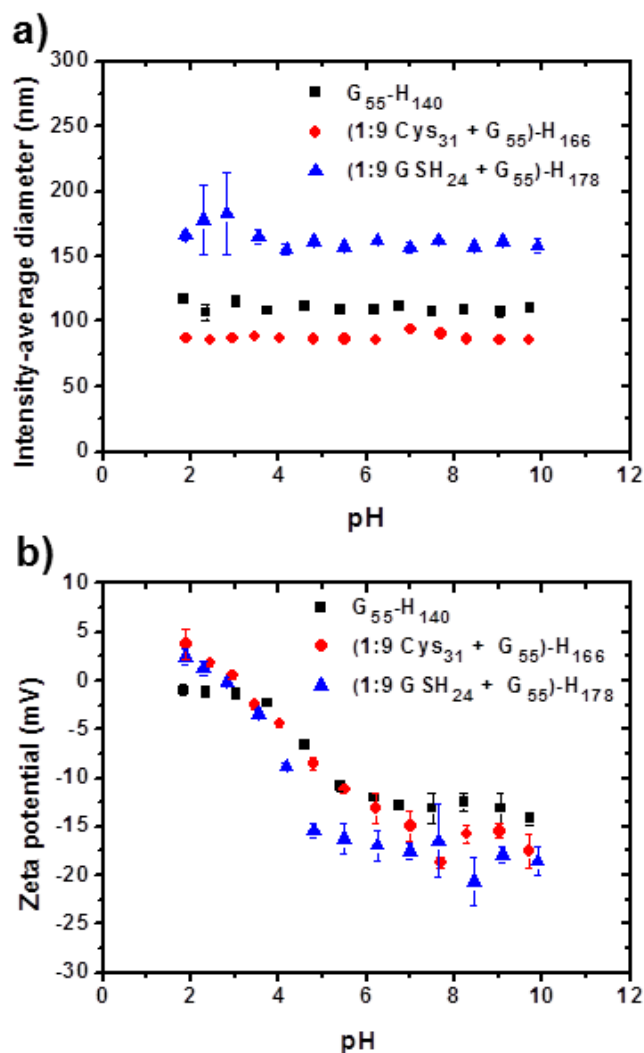

Figure 7. Variation of zeta potential and intensity-average diameter with pH for worms. (a) Intensity-average diameter vs pH for PGMA$_{55}$-PHPMA$_{140}$ (black squares), (1:9 PCysMA$_{31}$ + PGMA$_{55}$)-PHPMA$_{166}$ (red circles), and (1:9 PGSHMA$_{24}$ + PGMA$_{55}$)-PHPMA$_{178}$ (blue triangles). (b) Zeta potential vs. pH curves obtained for the same diblock copolymer dispersions. G, H, Cys and GSH designate PGMA, PHPMA, PCysMA and PGSHMA respectively.

The aqueous solution behavior of diblock copolymer nano-objects prepared using binary mixtures of macro-CTAs was then examined. Figure 7 shows the variation of intensity-average diameter and zeta potential with pH for worm formulations. The corresponding data for spheres and vesicles are shown in Figure S11. All three types of nano-objects remained colloidally stable between pH 2 and pH 10, with the presence of the non-ionic PGMA stabilizer chains preventing aggregation even at the IEP. Nano-objects prepared using the PGMA$_{55}$ macro-CTA alone remained weakly anionic over the entire pH range, presumably because of the carboxylic acid end-group originating from PETTC (or the ACVA initiator). In contrast, nano-objects containing either PCysMA$_{31}$ or PGSHMA$_{24}$ became weakly cationic below pH 2-3. More specifically, diblock copolymer nano-objects prepared using (1:9 PCysMA$_{31}$ + PGMA$_{55}$) or (1:9 PGSHMA$_{24}$ + PGMA$_{55}$) binary mixtures of macro-CTAs became cationic below pH 2.5-3, but acquired anionic character at higher pH (as observed for purely PGMA-stabilized nano-objects : PGMA$_{55}$-PHPMA$_{140}$, see Figure 7; as well as PGMA$_{55}$-PHPMA$_{100}$ and

PGMA$_{55}$-PHPMA$_{230}$, see Figure S11). In the case of nano-objects prepared from (1:9 PGSHMA$_{24}$ + PGMA$_{55}$) macro-CTA binary mixtures, this anionic character is significantly greater than that observed using a PGMA macro-CTA alone. Using macro-CTA binary mixtures enables the production of a wide range of well-defined, amino acid-functionalized diblock copolymer nano-objects with pH-dependent surface charge.

Conclusions

In summary, cysteine- and glutathione-containing methacrylic monomers (CysMA and GSHMA) have been synthesized on a multi-gram scale in high yield in aqueous solution at room temperature with minimal work-up. CysMA and GSHMA were polymerized in turn using RAFT polymerization to produce well-defined macro-CTAs. These macro-CTAs were used for the aqueous RAFT dispersion polymerization of 2-hydroxypropyl methacrylate to generate a wide range of diblock copolymer nano-objects at high solids in aqueous solution via polymerization-induced self-assembly. The zwitterionic PCysMA macro-CTA led to well-defined spheres, worms and vesicles, whereas the anionic PGSHMA macro-CTA only yielded spheres. However, using binary mixtures of these macro-CTAs in combination with a non-ionic PGMA macro-CTA enabled either spheres, worms or vesicles to be targeted as pure phases. Detailed phase diagrams were constructed to assist reproducible syntheses. Aqueous dispersions of either spheres or vesicles formed free-flowing liquids, whereas the worm dispersions formed free-standing temperature-sensitive gels. Rheological studies confirmed that the worm-like vesicles underwent a reversible worm-to-sphere transition on cooling, leading to degelation. Finally, these nano-objects exhibited complex electrophoretic behavior which appears to be governed by the chemical composition and nature of the steric stabilizer chains.

Notes and references

^{a} Institut Charles Gerhardt de Montpellier (UMR 5253, CNRS-UM2-ENSCM-UM1) ENSCM, 8, rue de l'école normale, 34296 Montpellier, France.

^{b} CEA Marcoule, DEN/MAR/DTCD/SPDE/LPSD, BP17171, 30207 Bagnols-sur-Cèze, France.

^{c} Institut Européen des Membranes (UMR 5635, ENSCM-CNRS-UM2), Université Montpellier 2, C.C. 047, Place E. Bataillon, 34095 Montpellier Cedex 05, France.

^{d} Department of Chemistry, University of Sheffield, Brook Hill, Sheffield, South Yorkshire, S3 7HF, UK.

* vincent.ladmiral@enscm.fr; s.p.armes@sheffield.ac.uk

Electronic Supplementary Information (ESI) available: Assigned NMR spectrum and titration curve for GSHMA monomer, GPC chromatograms for PCySMA$_{31}$, PGSHMA$_{24}$ and PGMA$_{55}$, kinetic data for RAFT polymerization of CysMA, additional phase diagram, further TEM images, G' and G'' vs. temperature curves, DLS studies of thermo-responsive worm gels, further zeta potential data vs pH obtained for spheres, worms and vesicles. See DOI: 10.1039/b000000x/

1   (a) M. G.Ryadnov, D.N. Woolfson, *Nature Mater.* 2003, **2**, 329. (b) R. A.Broglia, G. Tiana, D. Provasi, *J. Phys.: Condens. Matter* 2004, **16**, R111–R144. (c) J. R. Desjarlais, T. M. Handel, *Curr. Opin. Biotech.* 1995, **6**, 460. (d) G. Tuchscherer, L. Scheibler, P. Dumy, M. Mutter, *Biopolymers* 1998, **47**, 63.

2   J-F. Lutz, *Polym. Chem.*, 2010, **1**, 55.

3   D. Zhang, S. H. Lahasky, L. Guo, C-U. Lee, M. Lavan, *Macromolecules* 2012, **45**, 5833.

4   (a) H. R. Kricheldorf, *Angew. Chem. Int. Ed.* 2006, **45**, 5752. (b) H. Schlaad, M. Antonietti, *Eur. Phys. J.* 2003, **E 10**, 17,

5   T. J. Deming, *Nature*, 1997, **390**, 386.

6   (a) R. Hoogenboom, H. Schlaad, *Polymers* 2011, **3**, 467. (b) D. Kedracki, P. Maroni, H. Schlaad, C. Vebert-Nardin, *Adv. Funct. Mater.* 2014, **24**, 1133.

7   F. Sanda, T. Endo, *Macromol. Chem. Phys.* 1999, **200**, 2651.

8   A. Bentolila, I. Vlodavsky, R. Ishai-Michaeli, O. Kovalchuk, C. Haloun, A. J. Domb, *J. Med. Chem.* 2000, **43**, 2591.

9   R. K. Kulkarni, H. Morawetz, *J. Polym. Sci.* 1961, **54**, 491.

10   T. E. Hopkins, K. B.Wagener, *Adv. Mater.* 2002, **14**, 1703.

11   J.Morcellet-Sauvage, M. Morcellet, C. Loucheux, *Makromol. Chem.* 1981, **182**, 949.

12   M. Morcellet, C. Loucheux, H. Daoust, *Macromolecules* 1982, **15**, 890.

13   J. Morcellet-Sauvage, M. Morcellet, C. Loucheux, *Makromol. Chem.* 1982, **183**, 821.

14   J. Morcellet-Sauvage, M. Morcellet, C. Loucheux, *Makromol. Chem.* 1982, **183**, 831.

15   C. Methenitis, J. Morcellet-Sauvage, M. Morcellet, *Polym. Bull.* 1984, **12**, 133.

16   C. Methenitis, J. Morcellet-Sauvage, M. Morcellet, *Polym. Bull.* 1984, **12**, 141.

17   A. Lekchiri, J. Morcellet, M. Morcellet, *Macromolecules* 1987, **20**, 49.

18   C. Methenitis, J. Morcellet, M. Morcellet, *Eur. Polym. J.* 1987, **23**, 287.

19   C. Methenitis, J. Morcellet, G. Pneumatikakis, M. Morcellet, *Macromolecules* 1994, **27**, 1455.

20   F. Sanda, M. Nakamura, T. Endo, T. Takata, H Handa, *Macromolecules* 1994, **27**, 7928.

21   F. Sanda, M. Nakamura, T. Endo, *J. Polym. Sci., Part A: Polym. Chem.* 1998, **36**, 2681.

22   F. Sanda, M. Nakamura, T. Endo, *Macromolecules* 1996, **29**, 8064.

23   F. Sanda, T. Abe, T. Endo, *J. Polym. Sci., Part A: Polym. Chem.* 1997, **35**, 2619.

24   H. Murata, F. Sanda, T. Endo, *Macromolecules* 1996, **29**, 5535.

25   H.Murata, F. Sanda, T. Endo, *Macromolecules* 1997, **30**, 2902.

26   H. Murata, F. Sanda, T. Endo, *J. Polym. Sci., Part A: Polym. Chem.* 1998, **36**, 1679.

27   F. Sanda, F. Ogawa, T. Endo, *Polymer* 1998, **39**, 5543.

28   F. Sanda, J. Kamatani, H. Handa, T. Endo, *Macromolecules* 1999, **32**, 2490.

29   H. Kudo, F. Sanda, T. Endo, *Macromol. Chem. Phys.* 1999, **200**, 1232.

30   S. M. Bush, M. North, *Polymer* 1996, **37**, 4649.

31   S. M. Bush, M. North, *Polymer* 1998, **39**, 933.

32   S. M. Bush, M. North, S. Sellarajah, *Polymer* 1998, **39**, 2991.

Polymer Chemistry Accepted Manuscript

33 A. Birchall, S. M. Bush, M.; North, *Polymer* 2001, **42**, 375.

34 R. K. O'Reilly, *Polym. Int.* 2010, **59**, 568.

35 H. Mori, T. Endo, T. *Macromol. Rapid Commun.* 2012, **33**, 1090.

36 S. C. G. Biagini, R. Gareth Davies, V. C. Gibson, M. R. Giles, E. L. Marshall, M. North, *Polymer* 2001, **42**, 6669.

37 S. Sutthasupa, F. Sanda, T. Masuda, *Macromolecules* 2009, **42**, 1519.

38 S. Sutthasupa, M. Shiotsuki, H. Matsuoka, T. Masuda, F. Sanda, *Macromolecules* 2010, **43**, 1815.

39 I-D. Chung, P. Britt, D. Xie, E. Harth, J. M. Mays, *Chem. Commun.* 2005, **8**, 1046.

40 B. S. Lokitz, A. J Convertine, R. G. Ezell, A. Heidenreich, Y. Li, C. L. McCormick, *Macromolecules* 2006, **39**, 8594.

41 B. S. Lokitz, J. E. Stempka, A. W. York, Y. Li, H. K. Goel, G. R. Bishop, C. L. McCormick, *Aust. J. Chem.* 2006, **59**, 749.

42 M. G. Kellum, A. E. Smith, S. K. York, C. L. McCormick, *Macromolecules* 2010, **43**, 7033.

43 M. G. Kellum, C. A. Harris, C. L. McCormick, S. E. Morgan, *J. Polym. Sci., Part A: Polym. Chem.* 2011, **49**, 1104.

44 H. Mori, K. Sutoh, T. Endo, *Macromolecules* 2005, **38**, 9055.

45 H. Mori, M. Matsuyama, K. Sutoh, T. Endo, *Macromolecules* 2006, **39**, 4351.

46 H. Mori, M. Matsuyama, T. Endo, *Macromol. Chem. Phys.* 2008, **209**, 2100.

47 H. Mori, H. Iwaya, A. Nagai, T. Endo, C*hem. Commun.* 2005, **38**, 4872.

48 H. Mori, H. Iwaya, T. Endo, *React. Funct. Polym.* 2007, **67**, 916.

49 H. Mori, H. Iwaya, T. Endo, *Macromol. Chem. Phys.* 2007, **208**, 1908.

50 H. Mori, I. Kato, M. Matsuyama, T. Endo, *Macromolecules* 2008, **41**, 5604.

51 H. Mori, M. Matsuyama, T. Endo, *Macromol. Chem. Phys.* 2009, **210**, 217.

52 H. Mori, I. Kato, T. Endo, *Macromolecules* 2009, **42**, 4985.

53 H. Mori, I. Kato, S. Saito, T. Endo, *Macromolecules* 2010, **43**, 1289.

54 J. Du, H. Willcock, N. S. Ieong, R. K. O'Reilly, *Aust. J. Chem.* 2011, **64**, 1041.

55 J. Du, R. K. O'Reilly, *Macromol. Chem. Phys.* 2010, **211**, 1530.

56 J. Skey, H. Willcock, M. Lammens, F. Du Prez, R. K. O'Reilly, *Macromolecules* 2010, **43**, 5949.

57 J. Skey, R. K. O'Reilly, *J. Polym. Sci., Part A: Polym. Chem.* 2008, **46**, 3690.

58 J. Skey, C. F. Hansell, R. K. O'Reilly, *Macromolecules* 2010, **43**, 1309.

59 A. C. Evans, A. Lu, C. Ondeck, D. A. Longbottom, R. K. O'Reilly, *Macromolecules* 2010, **43**, 6374.

60 A. C. Evans, J. Skey, M. Wright, W. Qu, C. Ondeck, D. A. Longbottom, R. K. O'Reilly, *J. Polym. Sci., Part A: Polym. Chem.* 2009, **47**, 6814.

61 A. Lu, T. P. Smart, T. H. Epps, III, D. A. Longbottom, R. K. O'Reilly, *Macromolecules* 2011, **44**, 7233.

62 A. Lu, D. Moatsou, D. A. Longbottom, R. K. O'Reilly, *Chem. Sci.* 2013, **4**, 965.

63 A. Lu, P. Cotanda, J. P. Patterson, D. A. Longbottom, R. K. O'Reilly, *Chem. Commun.* 2012, **48**, 9699.

64 Y. Mai, A. Eisenberg, *Chem. Soc. Rev.* 2012, **41**, 5969.

65 L. F. Zhang, A. Eisenberg, *Science* 1995, **268**, 1728.

66 Y. Geng, P. Dalhaimer, S. S. Cai, R. Tsai, M. Tewari, T. Minko, D. E. Discher, *Nat. Nanotechnol.* 2007, **2**, 249.

67 Y. Y. Won, H. T. Davis, F. S. Bates, *Science* 1999, **283**, 960.

68 B. M. Discher, Y. Y. Won, D. S. Ege, J. C. M. Lee, F. S. Bates, D. E. Discher, D. A. Hammer, *Science* 1999, **284**, 1143.

69 D. E. Discher, A. Eisenberg, A. *Science* 2002, **297**, 967.

70 J. Rodriguez-Hernandez, S. Lecommandoux, *J. Am. Chem. Soc.* 2005, **127**, 2026.

71 G. Riess, *Prog. Polym. Sci.* 2003, **28**, 1107

72 H-C. Kim, S-M. Park, W. D. Hinsberg, *Chem. Rev.* 2010, **110**, 146.

73 M. C. Orilall, U. Wiesner, *Chem. Soc. Rev.* 2011, **40**, 520.

74 D. M. Vriezema, M. Comellas Aragonès, J. A. A. W. Elemans, J. J. L. M. Cornelissen, A. E. Rowan, R. J. M. Nolte, *Chem. Rev.* 2005, **105**, 1445.

75 J. Z. Du, Y. P. Tang, A. L. Lewis, S. P. Armes, *J. Am. Chem. Soc.* 2005, **127**, 17982.

76 K. Kita-Tokarczyk, J. Grumelard, T. Haefele, W. Meier, *Polymer* 2005, **46**, 3540.

77 (a) C. Giacomelli, V. Schmidt, K. Aissou, R. Borsali, *Langmuir*, 2010, **26**, 15734. (b) F. H. Schacher, P. A. Rupar, I. Manners, *Angew. Chem. Int. Ed.* 2012, **51**, 7898.

78 (a) Y. Li, S. P. Armes, *Angew. Chem., Int. Ed.* 2010, **49**, 4042. (b) A. Blanazs, J. Madsen, G. Battaglia, A. J. Ryan, S. P. Armes, *J. Am. Chem. Soc.* 2011, **133**, 16581. (c) S. Sugihara, A. Blanazs, S. P. Armes, A. J. Ryan, A. L. Lewis, *J. Am. Chem. Soc.* 2011, **133**, 15707. (d) M. Semsarilar, V. Ladmiral, A. Blanazs, S. P. Armes, *Langmuir* 2012, **28**, 914. (e) M. Semsarilar, V. Ladmiral, A. Blanazs, S. P. Armes, *Langmuir*, 2013, **29**, 7416. (f) V. Ladmiral, M. Semsarilar, I. Canton, S. P. Armes *J. Am. Chem. Soc.* 2013, **135**, 13574. (g) L. P. D. Ratcliffe, A. J. Ryan, S. P. Armes, *Macromolecules* 2013, **46**, 769. (h) N. J. Warren, O. O. Mykhaylyk, D. Mahmood, A. J. Ryan, S. P. Armes, *J. Am. Chem. Soc.* 2014, **136**, 1023.

79 (a) E. R. Jones, M. Semsarilar, A. Blanazs, S. P. Armes, *Macromolecules* 2012, **45**, 5091. (b) S. Boissé, J. Rieger, K. Belal, A. Di-Cicco, P. Beaunier, M-H. Li, B. Charleux, *Chem. Comm.* 2010, **46**, 1950. (c) X. Zhang, S. Boissé, W. Zhang, P. Beaunier, F. D'Agosto, J. Rieger, B. Charleux, *Macromolecules* 2011, **44**, 4149. (d) W. Cai, W. Wan, C. Hong, C. Huang, C-Y. Pan, *Soft Matter* 2010, **6**, 5554. (e) W-D. He, X-L. Sun, W-M. Wan, C-Y. Pan, *Macromolecules* 2011, **44**, 3358. (f) L. A. Fielding, M. J. Derry, V. Ladmiral, J. Rosselgong, A. M. Rodrigues, L. P D. Ratcliffe, S. Sugihara, S. P. Armes, *Chem. Sci.*, 2013, **4**, 2081. (g) S. Boissé, J. Rieger, G. Pembouong, P. Beaunier, B. Charleux, *J. Polym. Sci., Part A: Polym. Chem.* 2011, **49**, 3346.

80 H. Kudo, F. Sanda, T. Endo, *J. Polym. Sci., Part A: Polym. Chem.* 2001, **39**, 23.

81 L. Lotti, S. Coiai, F. Ciardelli, M. Galimberti, E. Passaglia, *Macromol. Chem. Phys.* 2009, **210**, 1471.

82 S. Zhang, J. Zou, F. Zhang, M. Elsabahy, S. E. Felder, J. Zhu, D. J. Pochan, K. L. Wooley, *J. Am. Chem. Soc.* 2012, **134**, 18467.

83 J. W. Chan, C. E. Hoyle, A. B. Lowe, M. Bowman, *Macromolecules* 2010, **43**, 6381.

84 (a) J. R. McKee, V. Ladmiral, J. Niskanen, H. Tenhu, S. P. Armes, *Macromolecules* 2011, **44**, 7692. (b) J. Mazzolini, O. Boyron, V.

Monteil, F. D'Agosto, C. Boisson, G. C. Sanders, J. P. A. Heuts, R. Duchateau, D. Gigmes, D. Bertin, *Polym. Chem.* 2012, **3**, 2383.

85 J. N. Israelachvili, D. J. Mitchell, B. W. Ninham, *J. Chem.Soc., Faraday Trans. 2*, 1976, **72**, 1525.

86 M. Antonietti, S. Förster, *Adv. Mater.* 2003, **15**, 1323.

87 A. Blanazs, R. Verber, O. O. Mykhaylyk, A. J. Ryan, J. Z. Heath, C. W. I. Douglas, S. P. Armes, *J. Am. Chem. Soc.* 2012, **134**, 9741.

88 C. A. Dreiss, *Soft Matter* 2007, IG, 956.

89 J. Madsen, S. P. Armes, A. L. Lewis, *Macromolecules* 2006, **39**, 7455.

90 A. M. Alswieleh, N. Cheng, I. Canton, B. Ustbas, X. Xue, V. Ladmiral, S. Xia, R. E. Ducker, O. El Zubir, M. L. Cartron, C. N. Hunter, G. J. Leggett, S. P. Armes *J. Am. Chem. Soc.*, 2014, **136**, 9404

91 K. L. Thompson, E. S. Read, S. P. Armes, *Polymer Degradation and Stability* 2008, **93**, 1460.